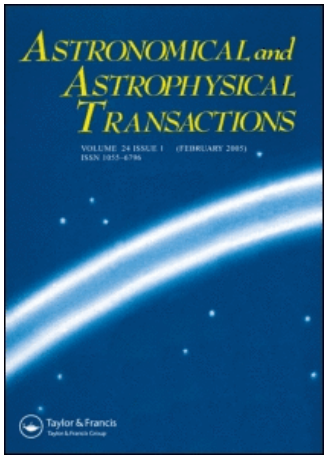

Astronomical & Astrophysical Transactions
The Journal of the Eurasian Astronomical Society
Publication details, including instructions for authors and subscription information:
http://www.informaworld.com/smpp/title~content=t713453505

DETECTION OF SEVERAL DAEMON POPULATIONS IN EARTH-CROSSING ORBITS

E. M. Drobyshevski [a]; M. V. Beloborodyy [a]; R. O. Kurakin [a]; V. G. Latypov [a]; K. A. Pelepelin [a]
[a] Ioffe Physical-Technical Institute, Russian Academy of Sciences, 194021 St Petersburg, Russia.

Online Publication Date: 01 February 2003
To cite this Article: Drobyshevski, E. M., Beloborodyy, M. V., Kurakin, R. O., Latypov, V. G. and Pelepelin, K. A. (2003) 'DETECTION OF SEVERAL DAEMON POPULATIONS IN EARTH-CROSSING ORBITS', Astronomical & Astrophysical Transactions, 22:1, 19 - 32
To link to this article: DOI: 10.1080/1055679081000080357
URL: http://dx.doi.org/10.1080/1055679081000080357

Astronomical and Astrophysical Transactions,
2003, Vol. 22(1), pp. 19–32

DETECTION OF SEVERAL DAEMON POPULATIONS IN EARTH-CROSSING ORBITS

E. M. DROBYSHEVSKI*, M. V. BELOBORODYY, R. O. KURAKIN,
V. G. LATYPOV and K. A. PELEPELIN

Ioffe Physical-Technical Institute, Russian Academy of Sciences, 194021 St Petersburg, Russia

(Received 1 July 2002)

Experiments on scintillator-based detection of negative dark electric matter objects, daemons, representing Planckian supermassive (about 2×10^{-5} g) particles that were detected in March 2000 as populating near-Earth, almost circular heliocentric orbits (NEACHOs), are being continued. The NEACHO objects hit the Earth with a velocity of about 10–15 km s^{-1}. The results of these and new experiments (April–June 2001) are now being processed, taking into account the difference in scintillation signal shape depending on the magnitude and sign of the velocity of the daemons crossing our detector, which was purposefully made asymmetric with respect to the up–down direction of flight. The data accumulated during the experiment and processed in this way also reveal the presence of, firstly, a high-velocity (about 35–50 km s^{-1}) daemon population whose objects can be related to a population in the Galactic disc and/or that in strongly elongated Earth-crossing heliocentric orbits and, secondly, a low-velocity (about 3–10 km s^{-1}) population in geocentric Earth-surface-crossing orbits whose objects (GESCOs) traverse repeatedly the Earth, suffering a decrease in velocity by about 30–40% month in the process.

The evolutionary relation between all these three (four?) populations is discussed. Conjectures concerning their manifestations in further observations are put forward.

An analysis of possible interaction processes of daemons, which may have different velocities and directions of motion, with the detector components (ZnS(Ag) scintillator layers, tinned-iron sheets 0.3 mm thick, etc.) on the atomic (emission of Auger electrons) and nuclear (nucleon evaporation from a nucleus excited in the capture and, subsequently, the decay of its protons) levels has permitted estimation of some characteristic times. In particular, the decay time of a daemon-containing proton was found to be about 1 μs.

Keywords: Detection of dark matter objects; Dark matter in the Solar System; Elementary black holes

1 INTRODUCTION: DESCRIPTION OF THE DETECTOR AND THE RESULTS OF THE FIRST EXPERIMENTS

We believe a substantial part of the Galactic disc dark matter (DM) to be made up of dark electric matter objects, daemons (Drobyshevski, 1996). They are relic elementary black holes moving with astronomical velocities and having mass of a Planckian scale, $M \approx 2 \times 10^{-5}$ g. It may be conjectured that the evolution of their ensemble with the initial spectrum close to the δ function had favored at the time the appearance of the baryon asymmetric visible matter (Barrow *et al.*, 1992) and further the formation of the large-scale struc-

* Corresponding authors: Email: emdrob@pop.ioffe.rssi.ru

ISSN 1055-6796 print; ISSN 1476-3540 online
DOI: 10.1080/1055679081000080357

ture of the Universe as we know it, for example quasars, and (super)clusters of galaxies with their (active) nuclei and spiral arms. The Planckian mass allows these black holes to have an electric charge of up to $Z \approx 10e$ (Markov, 1965). Negative daemons are nuclear-active particles. In building up inside the Sun, they are able to catalyse proton fusion, which may account for the observed solar energetics and the deficiency in the emitted neutrinos (Drobyshevski, 1996).

As the Sun captures daemons by slowing down their motion, some of them, acted upon by the gravitational perturbations by the Earth, should also populate strongly elongated Earth-crossing heliocentric orbits (SEECHOs) (Drobyshevski, 1997a; 2000b). Some of them transfer in due cause to near-Earth, almost circular heliocentric orbits (NEACHOs), from which they can then be transferred by the Earth into geocentric orbits crossing its surface (Drobyshevski, 2001; 2002).

Estimates showed (Drobyshevski, 1997a) that the volume concentration of daemons in SEECHOs exceeds that in the Galactic disc by a factor of about 10^3–10^5. Therefore, in contrast with the standard practice adopted when searching for the Galactic halo DM objects moving with velocities of 200–300 km s^{-1} (see for example Bauer (1998) and Spooner (1998)), our experiments were aimed from the very beginning at looking for a relatively low-velocity (35–50 km s^{-1}), but high-density population in SEECHOs. We planned to make use of the active interaction of negative daemons with atomic nuclei, including the decay of a daemon-containing proton in a time $\Delta\tau_{ex} \approx 10^{-7}$–$10^{-6}$ s (Drobyshevski, 2000a,b).

We developed a simple four-module detector (Drobyshevski, 2001; 2002). Each module contains two transparent polystyrene plates arranged horizontally one above the other at a distance of 7 cm. They are 4 mm thick and measure 50 cm × 50 cm. The plates were coated on the downside with an approximately 3.5 mg cm^{-2} layer of ZnS(Ag) powder with an average grain size of about 12 μm. Each plate was viewed by its photomultiplier (PM) tube. The plates were mounted at the centre of a cubic box, with a side of 51 cm, made of iron sheet 0.3 mm thick faced on both sides with a tin layer 2 μm thick.

The upper cover of the box was black paper. As will be seen later, all the components of the detector served to various degrees as its active elements.

The signals from each pair of the PM tubes were fed into a dual-trace digital storage oscillograph, which recorded them with a lead or delay of ±100 μs when triggered by a signal from the upper PM tube. If signals shifted relative to one another appeared on both traces, they were fed into a computer for subsequent processing.

The experiments were originally targeted to detect the SEECHO population. We expected to find signals shifted by $\Delta t = 7\text{ cm}/(35\text{–}50\text{ km s}^{-1}) \approx 1.5\text{–}2$ μs. However, the 700 h exposure made in March 2000 revealed an excess of signals at a level of 3.8σ within the interval $+20\,\mu\text{s} < \Delta t < +40\,\mu\text{s}$, which corresponds to a downward flux of some objects (Fig. 1(c)); the most significant events were those having on the first trace fairly long signals characteristic of scintillations caused by heavy non-relativistic particles of the type of α particles (HPSs) (Drobyshevski, 2002). Retrospectively, we think we were very lucky to stumble across this significant feature during the very first month of observations. If we had not recognized it as such, we would hardly have had sufficient stimulus and persistence to continue our observations.

The position of the peak at $\Delta t \approx +30$ μs permitted us to estimate immediately the flux velocity as $V \approx 7\text{ cm}/30\,\mu\text{s} \approx 2.5\text{ km s}^{-1}$, which, taking into account the possible inclination of the trajectories, could be increased to about 5 km s^{-1}. There were grounds to conclude that we have detected particles trapped by the Earth from the SEECHO population into geocentric orbits crossing the Earth's surface (Drobyshevski, 2001).

A more comprehensive analysis of possible implications of daemon interaction with the box wall material, combined with the narrowness of the peak observed at $\Delta t =$

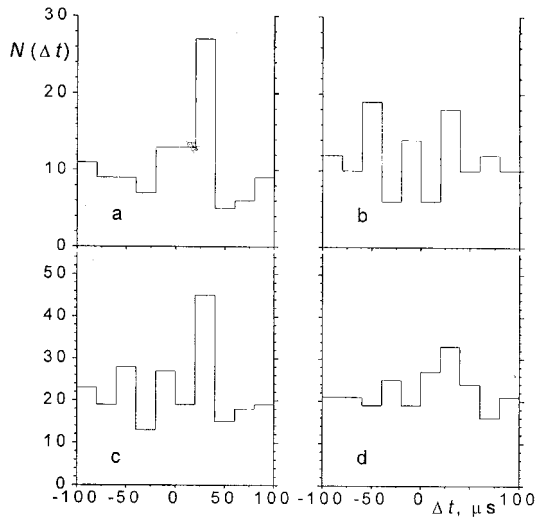

FIGURE 1 Statistics for shifted scintillations of upper and lower scintillators for February 24–March 27, 2000. Only heavy-particle scintillation (HPS) events at the upper scintillator, which activate the oscilloscopic sweep, are taken into account: (a) the 'wide' HPS distribution $N_w(\Delta t)$; (b) the 'narrow' HPS distribution $N_n(\Delta t)$ (for the definition $N_n(\Delta t)$ and $N_w(\Delta t)$ see Fig. 2 later); (c) the combined $N(\Delta t) = N_w + N_n$ demonstrating a sharp peak in $+20\,\mu s < \Delta t < 40\,\mu s$ bin; (d) the 'inverted' combined distribution $N_w(\Delta t) + N_n(-\Delta t)$, which shows the dependence of the HPS width on the up–down direction of the daemon motion and this dependence is most prominent for $\pm 20\,\mu s$ (see Fig. 3(d) also).

$+30 \pm 10\,\mu s$, suggested, however, that the weaker and shorter lower scintillations, primarily of the noise-like Scintillation (NLS) type, are due to numerous Auger electrons with energies of up to 0.6–1 MeV emitted in the capture of tin and iron atoms in the lower cover of the box, which corresponds to $V = (22\,cm + 7\,cm)/30\,\mu s = 10\,km\,s^{-1}$. Taking into account the trajectory inclinations within a solid angle of about $4\pi/6 = 2\,sr$ cut out by the side walls of the upper half of the box yields $V = 10$–$15\,km\,s^{-1}$. Such a velocity is characteristic of objects falling on the Earth from NEACHOs (Drobyshevski, 2002).

Section 2 will consider in more detail the processes accompanying the passage of a daemon through the components of our system.

Another problem which faced us was the strong seasonal variations in the daemon flux. We have to confess that initially we had believed the weak (about 7%) seasonal variations in the WIMP flux to be peculiar only to the Galactic halo population with $V \approx 200$–$300\,km\,s^{-1}$. We knew certainly that the Sun's velocity relative to the nearest stars is about $20\,km\,s^{-1}$ but assumed as a working hypothesis that the velocity relative to the nearest daemon background in the Galactic disc is, on average, negligible and small compared with the random velocity of the objects in this background. We did not intend to reach an accuracy in our measurements of better than 10%. As a result, on recording the above-mentioned maximum and carrying out a series of tests of the reliability of our measuring equipment we were surprised to find that the results obtained a couple of months later (a typical series of observations lasts about a month) very poorly reproduced the March 2000 data. This initiated a large number of improvements in the equipment and in its repeated tests, additional non-systematic experiments, attempts at devising another interpretation of their results (see for example Drobyshevski (2000c, 2001)), etc. At the same time we made gradual progress in understanding the character of the interaction of daemons with matter and their celestial mechanics and developed promising new techniques of data treatment (see Section 2). Therefore, when, at the very end of March 2001 we again started systematic observations and did not reveal a

maximum as significant as that found one year and a month before, we were not very much discouraged. A more sophisticated treatment of both old and new series of data accumulated during the period from April to June 2001 revealed new types of daemon population in the Solar System (Section 3) and their evolution with time (Section 4). This provided supportive evidence for the correctness of the strategy chosen by us, as well as the validity of the main ideas concerning the generic relation between the various daemon populations and their interaction with matter. As a result, we have been able to estimate the characteristic times of some processes occurring on atomic and subnuclear levels and, in particular, have obtained a more precise estimate of the decay time of the daemon-containing proton (Section 3). We certainly are aware of the fact that many important details of these processes still remain unclear and need a more comprehensive investigation (Section 3).

2 DETECTOR ASYMMETRY: ITS REASONS AND MERITS

As already mentioned, our detecting system was purposefully made asymmetric with respect to the up–down direction in order not only to reveal the very existence of daemons but also to broaden the scope of information concerning their properties and interaction with matter. The asymmetry was provided by depositing the ZnS(Ag) layer only on the downside of the polystyrene plates and by the lack of the top iron cover on the box. It was assumed that the upward-moving daemons would certainly be poisoned by heavy tin or iron nuclei, thus changing dramatically their properties, which would not happen with a downward flux, etc.

Table I gives some idea of the details of such processes. It presents path lengths λ of a super-massive particle with a negative charge charge $Z_{\text{eff}}e = 1e$ before it has recaptured an atomic nucleus, calculated for different substances (polystyrene, air, ZnS(Ag), iron and tin) at three characteristic velocities $V = 5$, 15 and 45 km s^{-1}. The choice of such a low value of Z_{eff} for the daemon is suggested by the totality of our experimental results, if for no other reason than that the characteristic times of flight in our system are, on the whole, fairly short compared with (or, at most, of the same order of magnitude as) the decay times of daemon-containing nuclei (and of the protons that they are made of). It is not inconceivable that sometimes one should adopt $Z_{\text{eff}} = 2$ or even $Z_{\text{eff}} = Z \approx 10$. It appears that large values (up to $Z_{\text{eff}} \approx 10$) may possibly be realized for a sufficiently long time only in large evacuated volumes. The cross-section for a (unexcited) nucleus with charge Z_{n} and mass Am_{p}, taking into account its displacement by a negative projectile, was determined from the expression (Drobyshevski, 2000b)

$$\sigma = \sigma_0 \frac{2Z_{\text{n}}e^2}{m_{\text{p}}R_0A^{4/3}} \frac{Z_{\text{eff}}}{V^2}, \tag{1}$$

where $\sigma_0 = \pi R_0^2 A^{2/3}$ and $R_0 = 1.2 \times 10^{-13}$ cm.

To assist in orienting oneself in the characteristic values of the quantities involved and to make possible their comparison, Table I presents also the dimensions l and the corresponding times t_l of flight for our system, as well as the Knudsen numbers $K = \lambda Z_{\text{eff}}/l$.

It would seem that, in crossing the tinned iron sheet of the box, a daemon should inevitably capture an iron nucleus, but slow daemons with $V \leq 10$–15 km s^{-1} will be poisoned by tin nuclei before that. By contrast, when daemons cross the ZnS(Ag) layer, a noticeable fraction of them, having velocities $V \geq 35$ km s^{-1}, may pass through without having interacted with a zinc or sulphur nucleus at all.

The asymmetry of the system should also affect the shape of the scintillations. It appears nearly obvious that a nucleus excited when captured in the ZnS(Ag) layer will not be able to evaporate all its nucleons in the de-excitation during the time that it takes to cross the thin

TABLE 1. Parameters of the Detector Components and Quantities Characterizing their Interactions with Daemons at Three Typical Velocities ($V = 5$, 15 and 45 km s^{-1}). l is the Component Size and t_l is Time that it is Traversed by Daemon; λ is the Mean Free Path Needed for a Daemon with $Z_{\text{eff}} = 1$ (the Most Probable Case) to Capture a Nucleus, τ_λ is the Corresponding Time (to Calculate λ and τ_λ, the Cross-Section Defined by Equation (1) is used). $K = \lambda Z_{\text{eff}}/l$ is the Knudsen Number.

	H	*C*	*Polystyrene*	*N*	*O*	*Air*		*S*	*Zn*	*ZnS(Ag)*	*Fe*	*Sn*
Z_n	1	6	CH	7	8			16	30		26	50
A	1	12		14	16			32	65		56	119
ρ ($g\,cm^{-3}$)	(0.082)	(0.978)	1.06	(0.00091)	(0.00028)	0.0012		(1.35)	(2.74)	4.09	7.9	7.3
l (cm)			0.4			7	22			10^{-3}	0.03	2×10^{-4}
t_l (μs)												
$v = 5$ km s^{-1}			0.8			14	44			2×10^{-3}	0.6	4×10^{-4}
$v = 15$ km s^{-1}			0.27			4.7	14.7			0.7×10^{-3}	0.02	1.3×10^{-4}
$v = 45$ km s^{-1}			0.09			1.6	4.9			2.2×10^{-4}	0.007	4.4×10^{-5}
λZ_{eff} (cm)												
$v = 5$ km s^{-1}	4.9×10^{-5}	5.2×10^{-5}	2.5×10^{-5}	5.1×10^{-2}	0.18	0.04		5.8×10^{-5}	5.1×10^{-5}	2.7×10^{-5}	1.6×10^{-5}	3.1×10^{-5}
$v = 15$ km s^{-1}	4.4×10^{-4}	4.7×10^{-4}	2.3×10^{-4}	4.6×10^{-1}	1.6	0.36		5.2×10^{-4}	4.5×10^{-4}	2.4×10^{-4}	1.4×10^{-4}	2.8×10^{-4}
$v = 45$ km s^{-1}	4.0×10^{-3}	4.2×10^{-3}	2.0×10^{-3}	4.1	14.5	3.2		4.7×10^{-3}	4.1×10^{-3}	2.2×10^{-3}	1.3×10^{-3}	2.5×10^{-3}
$\tau_\lambda Z_{\text{eff}}$ [ns]												
$v = 5$ km s^{-1}	0.1	0.1	0.05	102	360	80		0.12	0.10	0.054	0.032	0.062
$v = 15$ km s^{-1}	0.29	0.31	0.15	307	1070	240		0.35	0.30	0.16	0.093	0.19
$v = 45$ km s^{-1}	0.89	0.93	0.44	910	3200	710		1.04	0.91	0.49	0.29	0.56
$K = \lambda Z_{\text{eff}}/l$												
$v = 5$ km s^{-1}			6.3×10^{-5}			5.7×10^{-3}	1.8×10^{-3}			2.7×10^{-2}	5.3×10^{-4}	0.16
$v = 15$ km s^{-1}			5.6×10^{-4}			5.3×10^{-2}	1.6×10^{-2}			0.24	4.7×10^{-3}	1.4
$v = 45$ km s^{-1}			5×10^{-3}			0.45	0.15			2.17	4.3×10^{-2}	12.5

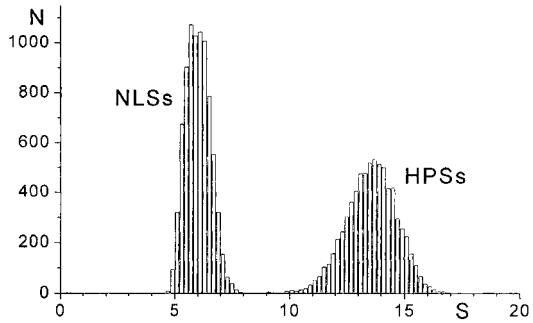

FIGURE 2 Typical distribution of the NLSs and HPSs *versus S*, the signal-amplitude normalized area swept by the oscilloscopic trace of the scintillation. These distributions can be approximated by Gaussians. The LPS and HPS distributions are well distinctive by their *S* values. The 'narrow' HPSs and 'wide' HPSs lie at the left and right-hand parts respectively of the HPS Gaussian.

luminophor layer. Therefore the HPSs produced by the nucleons evaporating in the polystyrene as the daemon moves upwards should be, on the average, shorter and weaker than that generated in its downward flight.

Figure 2 displays our data on the typical distributions of NLSs and HPSs plotted as a function of the area bounded by their oscilloscopic traces and normalized to the amplitude of the

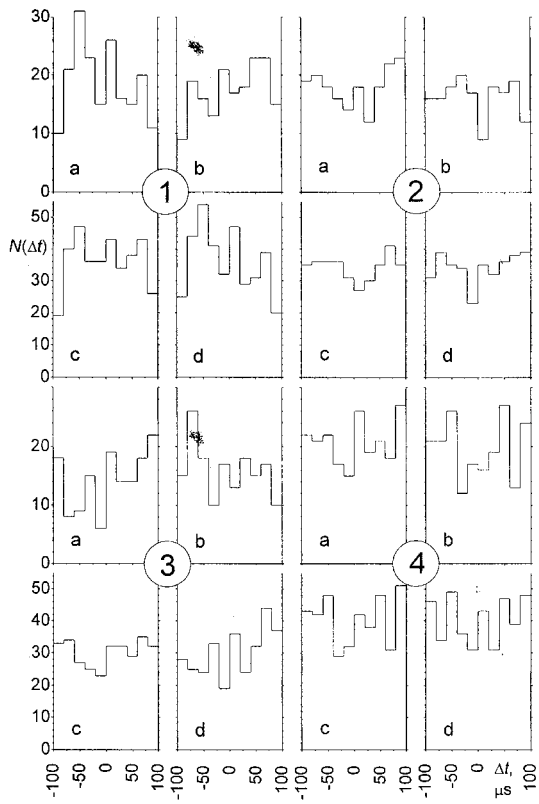

FIGURE 3 The same as for Figure 1 but for different time intervals in 2001: ① 30 March–25 April (590 h · m^2); ② 25 April–24 May (666 h · m^2); ③ 24 May–15 June (700 h · m^2); ④ 15 June–30 June (760 h · m^2). Note that from 6 June and on the second 4-module detector was put into operation in parallel with the first one (the total detector area became 2 m^2).

signal. (In experiments in 2001, we no longer inserted an inductance into the PM tube load circuit as was done earlier (Drobyshevski, 2000c; 2002); now the signal is picked off from a resistance $R = 30\,\mathrm{k\Omega}$ connected to the PM anode through $R = 1.5\,\mathrm{k\Omega}$; the capacity of the cable feeding the PM tube output signal to the oscillograph is 110 pF.) The NLS and HPS distributions are seen to be clearly separated. They can be well fitted by Gaussians. It is also evident that both distributions are produced primarily by background signals. Nevertheless, in view of the above remark on the possible effect of the direction in which a daemon crosses the ZnS(Ag) layer on the scintillation shape it appeared only natural to compare the parts of the distribution $N(\Delta t) = N_{\mathrm{n}}(\Delta t) + N_{\mathrm{w}}(\Delta t)$ constructed for the events contained in the left-hand (N_{n}, 'narrow' HPSs) and the right-hand (N_{w}, 'wide' HPSs) wings of the HPS Gaussian. This comparison (see Fig. 1(a) and (b) and Fig. 3(a) and (b)) yielded very important information both on the processes accompanying the nucleus capture by a daemon and on the existence of fairly distinct daemon populations and their possible generic relation.

3 DAEMON POPULATIONS (FAMILIES)

3.1 The Fast Component of the Daemon flux and Estimation of $\Delta\tau_{\mathrm{ex}}$, the Decay Time of Daemon-Containing Proton

The first thing that strikes the eye in the histograms in Figures 1(a) and (b) and Figures 3(a) and (b) is the inverse ratios of the numbers of events contained in the two central bins ($\pm 20\,\mu\mathrm{s}$) for the 'narrow' $N_{\mathrm{n}}(\Delta t)$ and 'wide' $N_{\mathrm{w}}(\Delta t)$ parts of the HPS $N(\Delta t)$ distribution. The upward flux ($-20\,\mu\mathrm{s} \leq \Delta t \leq 0\,\mu\mathrm{s}$) generates a larger number of 'narrow' than 'wide' events compared with the downward-moving flux ($0\,\mu\mathrm{s} < \Delta t < +20\,\mu\mathrm{s}$). It is just what we expected to find (Drobyshevski, 2001; 2002) (see also Section 2) by assuming that the evaporative de-excitation time τ_{ev} of a captured nucleus exceeds noticeably the daemon flight time t_l through the ZnS(Ag) layer approximately 10 μm thick, and that particle evaporation from an upward-moving nucleus ends in the polystyrene (note that the mean free path of a 1 MeV α particle in polystyrene is about 20 μm). Hence it follows (see Tab. I) that $\tau_{\mathrm{ev}} \gtrsim 2 \times 10^{-10}\,\mathrm{s}$ (if a scintillator nucleus is captured at this velocity at all; see below). A downward-moving daemon-containing nucleus exiting ZnS(Ag) into air causes a fairly wide, 'normal' HPS.

The events falling in the $-20\,\mu\mathrm{s} < \Delta t < +20\,\mu\mathrm{s}$ bins are produced by daemons moving with velocities $15\,\mathrm{km\,s^{-1}} \lesssim V \lesssim 50\,\mathrm{km\,s^{-1}}$, if they are calculated on the basis of the distance from the lower box cover to the upper ZnS(Ag) layer. Taking this into account, the trajectory inclinations may increase V by a factor of 1.5–2, raising the lower limit of V, accordingly, at most by up to 20–30 $\mathrm{km\,s^{-1}}$. As for the upper bound on the velocity, a trial exclusion of the few events corresponding to $-2\,\mu\mathrm{s} \leq \Delta t \leq +2\,\mu\mathrm{s}$ from the central bins did not result in any significant change.

The data available to date permit a conclusion that we are observing objects populating SEECHOs ($V \approx 35$–$50\,\mathrm{km\,s^{-1}}$) and/or those of the interstellar background, that is of the Galactic disc population, if the Sun moves relative to it with $V \approx 10$–$20\,\mathrm{km\,s^{-1}}$ (then, taking into account the Earth's orbital motion, we again obtain $V_{\max} \approx (10\text{–}20) + V_{\oplus_{\mathrm{orb}}} \approx 35\text{–}50\,\mathrm{km\,s^{-1}}$). Measurements spanning even only 1 year would apparently be enough to discriminate between these two populations with good confidence. Thus, we may expect that in about half a year after the observations reported here, when $V_{\oplus_{\mathrm{orb}}}$ changes direction relative to the incoming flux from the Galactic disc, there will be a certain deficiency of events in the $-20\,\mu\mathrm{s} < \Delta t < +20\,\mu\mathrm{s}$ interval.

As seen from Table I, for $V \approx 35$–$50\,\mathrm{km\,s^{-1}}$ a daemon with $Z_{\mathrm{eff}} = 1$ crosses the 2 μm tin layer almost without capturing a tin nucleus but capturing with an approximately 100% probability an iron nucleus in the iron sheet 0.3 mm thick. The probability of capturing a sulphur or zinc nucleus in the ZnS(Ag) layer is about 50%.

The fact that the upward flux produces in the $-20\,\mu\mathrm{s} < \Delta t < +20\,\mu\mathrm{s}$ interval always more 'narrow' HPSs, and the downward flux produce, more 'wide' HPSs, permits the conclusion that in the first case in the time $\Delta t \leq 20\,\mu\mathrm{s}$ elapsing between the capture of an iron nucleus in the lower box cover and its entering the upper scintillator layer, some approximately $Z_n - 9 = 17$ protons are evaporated from the excited iron nucleus, While the remainder of these 17 protons become subsequently 'digested' by the daemon that it contains.

This estimate is obtained also for the downward flux of daemons, which capture sulphur or zinc in the upper scintillator layer and acquire, before reaching the lower box cover in $\Delta t \leq 20\,\mu\mathrm{s}$, an effective charge $Z_{\mathrm{eff}} \geq 1$, that is, an ability to capture in it an iron nucleus, with subsequent emission of high-energy (up to about 0.6–1 MeV) Auger electrons, which penetrate through the approximately 0.3 mm iron sheet and initiate (together with the δ electrons) a scintillation in the lower ZnS(Ag) layer.

Bearing in mind that the binding energy of a 'pure' daemon ($Z_{\mathrm{eff}} = Z = 10$) with a nucleus $A/2 \approx Z_{\mathrm{n}} = 9$ is as high as $W \approx 1.8 Z Z_{\mathrm{n}} A^{-1/3}\,\mathrm{MeV} \approx 62\,\mathrm{MeV}$ and that, with an iron nucleus ($Z_{\mathrm{n}} = 26$; $A = 56$) this gives $W \approx 122\,\mathrm{MeV}$, we obtain a value of about 60 MeV for the energy expended immediately to heat the iron nucleus newly captured in place of the nucleus with $Z_{\mathrm{n}} = 9$. If the average nucleon binding energy in a nucleus is about 7.5 MeV, this energy is high enough to evaporate, in $\tau_{\mathrm{ev}} \ll 20\,\mu\mathrm{s}$, about eight nucleons (or two or three α particles). As a consequence, the de-excited iron nucleus transforms to a nucleus with $Z_{\mathrm{n}} \approx 20$–$22$ (approximately the same values apply to zinc; the nucleus left over after the evaporation of nucleons in sulphur in τ_{ev} will have $Z_{\mathrm{n}} \approx 14$). After this, consecutive daemon decay of the 'excess' $Z_{\mathrm{n}} - Z_{\mathrm{eff}} = 21 - 9 = 12$ protons takes place in $\Delta t \leq 20\,\mu\mathrm{s}$. This yields $\Delta\tau_{\mathrm{ex}} \leq 20/12 \approx 1.7\,\mu\mathrm{s}$ for the decay of a daemon-containing proton.

3.2 Daemons in near-Earth Almost-circular Heliocentric Orbits

The $N(\Delta t)$ distribution accumulated in March 2000 exhibits a fairly narrow maximum at $\Delta t \approx +30 \pm 10\,\mu\mathrm{s}$ at a confidence level of about 99.9% (Fig. 1(c)). There is no symmetric counterpart to it for $\Delta t < 0$. Taking as a reference the distance $l = 29\,\mathrm{cm}$ between the upper scintillator and the lower box cover, we obtain (with due account of trajectory inclination within about 2 sr) a velocity $V \approx 10$–$15\,\mathrm{km\,s^{-1}}$. This value is in good agreement with the value expected for NEACHO objects falling on the Earth (Drobyshevski, 2002). The evolution of the heliocentric and other daemon populations is covered in more detail in Section 4.

At such a velocity, the probability for a daemon to capture a tin nucleus in the box walls is close to unity (see Tab. I), which accounts for the absence of signals due to the corresponding upward flux, as well as for the narrowness itself of the distribution ($\Delta t \approx +30 \pm 10\,\mu\mathrm{s}$), because the side walls of the upper half of the box cut out from above a solid angle of about 2 sr.

For $Z = 10$, the energy released in the capture of a tin nucleus, $W \approx 183\,\mathrm{MeV}$, which leaves about 120 MeV for the excitation of the tin nucleus and evaporation of its nucleons (for the initial $Z_{\mathrm{eff}} = 9$). This energy is large enough to evaporate about 16 nucleons, with about 40–42 protons left in the remaining nucleus. Hence it follows that $\Delta\tau_{\mathrm{ex}} \geq (30\,\mu\mathrm{s})/(41 - 9) \approx 0.9\,\mu\mathrm{s}$. Taking into account the data presented in Section 3.1, we find that $1.7\,\mu\mathrm{s} \geq \Delta\tau_{\mathrm{ex}} \geq 0.9\,\mu\mathrm{s}$.

In these estimates we disregard, on the one hand, the possibility that excitation energy is removed by γ-radiation and, on the other, that the nucleus ejects nucleon clusters.

Note also that the $+20\,\mu s < \Delta t < 40\,\mu s$ bin contains, to within statistical error, approximately equal numbers of the wide and narrow HPSs.

3.3 Low-velocity Orbit Population

3.3.1 Evidence for the Existence of a Geocentric Population.

It could be assumed that all daemons belong to the two (possibly, three) above-mentioned populations, and that beyond the $\Delta t = \pm 40\,\mu s$ interval the $N(\Delta t)$ population contains background signals only. A comparison of the $N_w(\Delta t)$ and $N_n(\Delta t)$ distributions in Figures 3①(a) and (b) shows, however, that the wide HPSs lie, as a rule, within $-80\,\mu s \leq \Delta t \leq -40\,\mu s$, and the narrow HPSs, within $+80\,\mu s \leq \Delta t \leq +40\,\mu s$. If these were purely background signals, there would be no such correlation with Δt. Thus, we have to admit that there is one more daemon population, whose upward flux initiates the wide HPSs, and the downward flux the narrow HPSs. This situation is the inverse of that with the SEECHO objects.

The April 2000 $N(\Delta t)$ distribution Figure 3①(c) exhibits two, nearly symmetric maxima at $\Delta t \approx -(40\text{–}80)\,\mu s$ and $\Delta t \approx +(40\text{–}80)\,\mu s$, which correspond to a velocity of 5–10 km s^{-1}. It appears only natural to assume that we observe here indeed a population in geocentric Earth-surface-crossing orbits (GESCOs). We believed earlier that it is the objects with $+20\,\mu s < \Delta t < +40\,\mu s$ that are due to this population (Drobyshevski, 2001; 2002).

For velocities not greater than 10 km s^{-1}, the 2 μm tin layer becomes, as we have seen, opaque to the capture of a tin nucleus. The maximum at $\Delta t < -40\,\mu s$ suggests that by this time the upward-moving daemons cause a tin nucleus to disintegrate to the extent where their (plus the daemon's $Z = 10$) charge becomes $Z_{eff} = 1$. Hence it follows, in accordance with the calculations made at the end of Section 3.2, that $\Delta\tau_{ex} \leq (40\,\mu s)/(41 - 9) \approx 1.3\,\mu s$. Recalling the estimates made in Section 3.2 and 3.1, we find that $\Delta\tau_{ex} \approx 0.9\text{–}1.3\,\mu s$.

This result follows directly from the difference in the behaviour of $N(\Delta t)$ observed to occur as Δt crosses the value $-40\,\mu s$. It certainly needs refining by taking into account the possible emission of γ quanta and nucleon clusters, more accurate calculation of the binding energies, etc. One may also conclude, in particular, that the 7 cm gap between the scintillators can be adopted as a reference only for the very-low-velocity daemons (not greater than 5 km s^{-1}), that is when their time of flight through this gap is longer than the time that the daemon needs to shed off (at least partially, to $Z_n < Z$) the nucleus that it had captured in the scintillator (see the end of Section 3.1 and Section 4).

3.3.2 On the Dependence of the Visible Manifestation of Scintillations on the Direction of Daemon Passage Through the Scintillator.

Now what could be the reason for the differences in the HPS width taking place as one crosses over from the high ($|\Delta t| \leq 20\,\mu s$) to medium ($20\,\mu s < |\Delta t| < 40\,\mu s$) velocities, where they are insignificant, and to lower velocities ($40\,\mu s \leq |\Delta t| \leq 80\,\mu s$), the situation where the upward-moving daemon, on capturing a zinc or tin nucleus, creates a longer scintillation observed by the upper PM tube than when it propagates downwards?

The fact is that an HPS initiated by a daemon capturing a nucleus is, generally speaking, the result of two processes. The first of these is the fast emission of many high-energy Auger electrons. They produce short NLSs. These NLSs are, however, immediately superimposed on by a series of true HPSs caused by evaporation from the nucleus of nucleons, likewise in large numbers.

When a slow enough ($40\,\mu s \leq |\Delta t| \leq 75\,\mu s$) upward-moving daemon (with $Z_{eff} = 1$) enters the bulk of the ZnS(Ag) layer and captures a nucleus, it emits tens of Auger electrons

during τ_{Aug}. If $\tau_{Aug} \ll t_l$, and the electron mean free path $\lambda_e \ll l$, the light produced in this NLS is also emitted from a layer of thickness about $\lambda_e \ll l$. Note that, for a 25 keV electron, $\lambda_e \approx 1\,mg\,cm^{-2}$ and, for a 50 keV electron, $\lambda_e \approx 4\,mg\,cm^{-2}$. Although some electrons are apparently emitted with energies of up to about 1 MeV, the maximum of their energy distribution may be expected to lie at low energies (possibly, at 1–10 keV). In order to reach the upper PM tube, the light from the lower part of the ZnS(Ag) layer has to cross almost the whole thickness $l - \lambda_e$ of this layer. It is known that, while the ZnS(Ag) phosphor is white, its transparency to its natural radiation is far from 100% because of scattering and absorption (Birks, 1964). The subsequent HPS radiation generated by the daemon-containing evaporating nucleus propagating through the remaining scintillator a layer (at $\tau_{ev} \approx t_l$), which is closer to the PM tube, has more favourable conditions to reach the latter.

Now the slow daemons moving downwards face the reverse situation. Here, the short NLS part of the scintillation is emitted in a thin (much less than l) layer facing the PM tube, and the longer HPS part in the remaining bulk of the light-scattering ZnS(Ag) layer. As a result, the total observed radiation will be, on average, shorter even if it seems to have the same amplitude.

For very slow daemons ($V \leq 5\,km\,s^{-1}$), whose transit time t_l through the ZnS(Ag) layer is substantially longer than $\tau_{Aug} + \tau_{ev}$, the situation of the scintillation shape changes again. In this case, the light from the scintillations excited successively by the Auger electrons and the evaporating nucleons should pass almost the same path length l in the ZnS(Ag) layer. As a result, both scintillation components will suffer the same attenuation, and the difference in the paths passed by light in the bulk of the ZnS(Ag) layer can no longer be used to discriminate between the two, as was the case with velocities in the approximate range $10\,km\,s^{-1} \leq V \leq 35\,km\,s^{-1}$. Therefore, as both wings of the $N(\Delta t)$ distribution obtained for $\Delta t \approx 60$–$70\,\mu s$ become progressively more filled because of the slowing down of the GESCO daemons, the differences between $N_w(\Delta t)$ and $N_n(\Delta t)$ first (for $V \to 5\,km\,s^{-1}$) level off (see Fig. 3②(a) and (b)), after which, for $|\Delta t| \geq 70$–$80\,\mu s$ ($V \leq 4\,km\,s^{-1}$), $N_w(\Delta t)$ even surpasses $N_n(\Delta t)$ (Fig. 3③(a) and (b)). This new reversal of the N_w/N_n ratio occurring for $\Delta t \geq 70$–$80\,\mu s$ can be accounted for if both parts of a scintillation (NLS and HPS) have about the same amplitude. In this case, the daemon scintillation will be slightly more filled than the standard background HPS, which is excited, for instance, by natural radioactivity. Obviously, the daemon-initiated scintillation will fall now into the right-hand part of the HPS Gaussian in Figure 2. Figure 4 displays the evolution of the average N_w/N_n ratio for daemon scintillations as a function of Δt. Because of a slightly weaker attenuation of scintillations due to the downward-moving daemons, they will be detected in somewhat larger numbers than the scintillations caused by the daemons moving upwards.

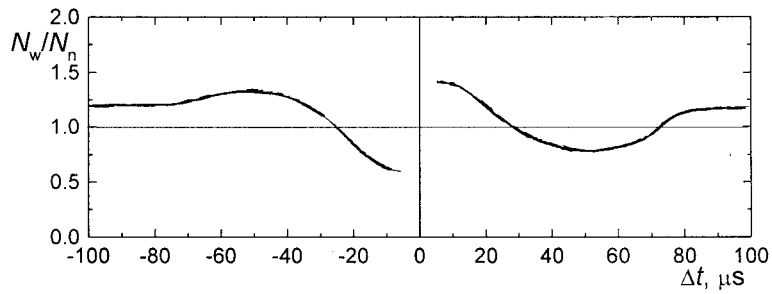

FIGURE 4 Schematic diagram of the dependence of the asymmetry of the HPSs caused by daemons on the time shift Δt of the upper and lower scintillations, that is of the daemon velocity (if distance between the upper scintillator and the bottom case cover is taken to be 29 cm).

As seen from Table I, in order for the scintillations to have the observed shape depending on the direction of the emitter motion in ZnS(Ag) (including the velocities of 35–50 km s^{-1}), the condition $\tau_{\mathrm{Aug}} \leq 10^{-10}$ s $< t_l$ should be met, and the time of evaporative nucleus de-excitation should be $\tau_{\mathrm{ev}} \approx 10^{-9}$ s (or slightly shorter). Because the shape of the daemon-initiated scintillations depends on Δt, the available statistics are not yet sufficient to discriminate reliably between the HPSs caused by daemons and by the background.

4 ON THE ORBITAL EVOLUTION OF DAEMONS IN HELIOCENTRIC AND GEOCENTRIC ORBITS

The fairly limited observational material presented above and its interpretation suggest already a certain pattern of the hierarchy of the near-solar daemon populations and of their possible evolution, which permits some predictions of the results that can be obtained in forthcoming experiments.

(i) The population of the Galactic disc has a velocity dispersion less than or equal to the velocity of motion of the Solar System relative to the disc. The opinion (see for example Freese *et al.*, (1988)) that at the beginning of June the average elliptical projection of the velocity vector of the Galactic halo population adds to the Earth's orbital velocity, and half a year later, at the beginning of December, is subtracted from it is apparently applicable to a degree to the Galactic disc population too.

(ii) Because of the Galactic disc daemons cross the Sun are slowed down, the Sun captures some of them (with $V_\infty \leq 20$ km s^{-1} (Drobyshevski, 1996)) into heliocentric orbits with perihelia lying inside it. Perturbations by the Earth transfer subsequently a few of these daemons into the SEECHOs with perihelia outside the Sun (Drobyshevski, 1997a). The SEECHO aphelia are oriented primarily in the direction of the 'shadow' created by the Sun in the incoming flow of the Galactic disc population. The Earth crosses this shadow in March (and, possibly, in February as well). Possibly, some of the already slowed-down daemons, which, in the course of their capture by the Sun, fall on it back from the shadow region and, on traversing the Sun, exit it from the opposite side to enter the 'antishadow' that is counter to the flow of the Galactic disc population, produces a weaker and diffuse 'antishadow' SEECHO population.

(iii) Multiple interactions of the Earth with the SEECHO objects transfer some of them gradually to NEACHOs (Drobyshevski, 2002). Because the SEECHOs and concentrated primarily in the 'shadow', the orbits of the NEACHO population should cross the Earth orbit (to be more precise, the torus swept by the Earth's sphere of influence) in the 'shadow' region. In this way a diverging beam of NEACHOs exiting the shadow region forms (a similar NEACHO focusing can occur in the region where the Earth's orbit crosses the antishadow). The daemons populating the NEACHOs fall on the Earth with a velocity of about 11.2–15 km s^{-1}. It is this flux that we detected in March 2000.

(iv) As a daemon repeatedly meets the Earth and traverses it, its velocity relative to the Earth decreases to the extent where it can be captured into the GESCOs. It is this population that produced the maxima at $\pm$50μs observed in April 2001 (Fig. 3①(c) and (d)). The fate of the daemons in GESCOs is clear; slowed down by the Earth, their velocity decreases gradually, and they drop below the Earth's surface. This scenario correlates fully with the spread-out and monotonic displacement of the maximum in $N(\Delta t)$ from $|\Delta t| \approx 50$ μs in April to $|\Delta t| \approx 60$–80 μs thereafter, from the end of May to June (compare Fig. 3①(c), 3②(c) 3③(c) and 3④(c)). Thus, the average GESCO daemon velocity at the Earth's surface decreases by about 30–40% in a month. This value offers

the possibility of estimating the force with which the Earth's matter slows down the daemons. Bearing in mind that the capture of nuclei of the matter by the daemon may result in $Z_{\text{eff}}\tau$ 0, an *ab initio* calculation of this force is not simple. Now, if we assume it to originate from momentum transfer to individual atoms (or their nuclei) in the daemon path, our experiments suggest that such interaction occurs, on average, on a path $\lambda_{\text{eff}} \approx 10^{-6}$–$10^{-5}$ cm, which is much larger than the internuclear distances in matter (about 10^{-8} cm).

(v) Because the probability of nuclear capture and excitation of a scintillation in our ZnS(Ag) detector about 10 μm thick drops below unity for velocities $V > 35\,\text{km s}^{-1}$, and, also, because τ_{Aug} is comparable with t_l, it appears only natural to assume that we detect far from all events produced by daemon moving with $V > 35\,\text{km s}^{-1}$. (Note that the system becomes transparent altogether for particles with $V > 50\,\text{km s}^{-1}$.) Therefore to arrive at the lowest limit for the daemon flux through our detector, we may justifiably assume that the $-20\,\mu\text{s} < \Delta t < 0\,\mu\text{s}$ bin the inverted $N_{\text{w}}(\Delta t) + N_{\text{n}}(-\Delta t)$ distribution (Fig. l(d) and Figs. 3①(d), 3②(d), 3③(d) and 3④(d)) may not practically contain daemon events, so that its level approaches that of the background. However, then the background events (approximately 20 ± 5 events per bin) constitute about 80–85% of the total number of all events. Hence the total downward flux in March 2000 is given by about 28 events, all of which belong to the $+20\,\mu\text{s} < \Delta t < 40\,\mu\text{s}$ bin. Thus, the average downward flux is $f_{\oplus} \geq 10^{-5}\,\text{m}^{-2}\,\text{s}^{-1}$. As already mentioned, the flux components vary in time.

The high-velocity component ($0\,\mu\text{s} < \Delta t < 20\,\mu\text{s}$), as evident from Figures 1 and 3, appears to present always; hence it follows that it is primarily due to the Galactic disc population. If it was the SEECHO population, we would also have always observed NEACHO daemons. The fraction of the high-velocity component is small, apparently both because it does not build up in NEACHOs and GESCOs and, possibly, because our system is transparent to daemons with high velocities (not less then 40–50 km s^{-1}).

While the differences in the numbers of events for the inverted distributions $N_{\text{w}}(\Delta t) + N_{\text{n}}(-\Delta t)$ within the $-20\,\mu\text{s} < \Delta t < 0\,\mu\text{s}$ and $20\,\mu\text{s} > \Delta t > 0\,\mu\text{s}$ bins are seen by eye, they become statistically significant only when the events of Figures 1(d), 3①(d), 3②(d), 3③(d) and 3④(d) are summed over the whole 4 month interval. One may assume the presence of seasonal variations; however, the data are still insufficient to reveal them.

The March distribution exhibits a flux with $V \approx 10$–$15\,\text{km s}^{-1}$ ($+20\,\mu\text{s} < \Delta t < 40\,\mu\text{s}$). Tested by the χ^2 criterion, the $N(\Delta t)$ distribution is not a constant level with a CL of about 99.99%. This flux is due to the NEACHO population. Some fraction of this population is captured into GESCOs, which becomes manifest in April in the appearance of two diffuse but statistically fairly significant maxima (see also the $N_{\text{w}}(\Delta t) + N_{\text{n}}(-\Delta t)$ sum in Fig. 3①(d)) lying at $-80\,\mu\text{s} < \Delta t < -40\,\mu\text{s}$ and $+40\,\mu\text{s} < \Delta t < +80\,\mu\text{s}$ (the difference from $N =$ constant has a CL of 95.8%).

Because of the gradual slowing down of the GESCO population, in the May $N(\Delta t)$ distribution these maxima spread out and shift towards larger $|\Delta t|$ to make the whole distribution within our $\Delta t = \pm 100\,\mu\text{s}$ limits filled well with a small dip at the centre (the CL with N not constant by the χ^2 criterion is only 9%). Because the events belonging to the side maxima of $N(\pm\Delta t)$ are displaced gradually to the $\Delta t = \pm 100\,\mu\text{s}$ limits, the central minimum begins to spread out, with a noticeable maximum appearing at its centre in the first half of June (Fig. 3③(c)) (as a result, the CL of $N(\Delta t)$ with N not constant starts again to increase and reaches 15% and even 85% in the second half of June; see Fig. 3④(c). The formation of this maximum may be associated with when the daemon flux from the Galactic disc becomes a maximum because its velocity adds to the Earth's orbital velocity. However, this maximum could possibly be caused by a gradual decrease in the GESCO population velocity

($V \leq 4\,\mathrm{km\,s^{-1}}$) (see Section 3.3.1). As a result, the 7 cm gap becomes basic because the time of traverse increases to a value which is sufficent for the captured nucleus to decay to $Z_n \leq 9$.

The net picture suggested by all these events is that some of the daemons which crossed our $1\,\mathrm{m}^2$ system in March with a time shift $+20\,\mu\mathrm{s} < \Delta t < 40\,\mu\mathrm{s}$ are captured into GESCOs. In April to June, they only diffuse in the velocity space and decrease in average velocity by about 30–40% per month.

In fact, all GESCO objects should eventually pass under the Earth's surface. The flux $f_\oplus \approx 10^{-5}\,\mathrm{m^{-2}\,s^{-1}}$ corresponds to $5 \times 10^9\,\mathrm{s^{-1}}$ daemons crossing the Earth's surface. Accepting that the period of revolution is about 5000 s along a GESCO, the total number of daemons trapped into the GESCOs in March and dropping gradually into the Earth will be about 2.5×10^{13}. (If this process of trapping is repeated in the solar antishadow half a year later, the latter figure doubles.) In 4.5×10^9 years, $2.5 \times 10^{13} \times 4.5 \times 10^9 \approx 10^{23}$ daemons have accumulated in the Earth, their total mass amounting to about $2 \times 10^{18}\,\mathrm{g}$ (Drobyshevski, 2001). We are not going to discuss their fate here.

For the rate of velocity decrease in the GESCOs found by us, most of them will escape under the Earth' surface half a year after capture. Therefore, at the end of summer, the GESCO aphelia are located near the Earth's surface, where the daemon velocity drops to very low levels. Considered in terms of the daemon hypothesis of ball lightning (Drobyshevski, 1997b), this would favour their formation, which may correlate with the highest frequency of their occurrence at this time of the year (about two thirds in July–August (Smirnov, 1990)).

5 CONCLUSION

Attempts at interpretation of the processes occurring in our seemingly simple scintillation detector show it to be in actual fact a fairly complex system. The detector was built specifically to reveal the passage through it of slow, electrically charged super-massive Planckian particles, the DM objects. In particular, the ideology underlying this system assumed from the outset the possibility of decay of a daemon-containing proton. Although the experiment has revealed a number of events that at first glance appeared strange, nevertheless most of them find a self-consistent qualitative interpretation within the framework of the daemon hypothesis and permit new conclusions on the properties and interaction of daemons with matter in general, and with the Sun and the planets. in particular.

It should be stressed that, irrespective of our understanding of the finer details of the processes occurring on the atomic and subnuclear levels, the results of the experiment imply unambiguously the existence of a flux of fairly slow long-living microscopic nuclear-active objects that possess a giant penetrating ability. It was assumed that it is these properties that would be characteristic of charged Planckian objects because of their huge mass.

The March 2000 observations revealed a daemon population in NEACHOs. They showed that the main information obtained by the detector is contained in the extended scintillations, similar to those produced by α particles. The high-velocity population (35–$50\,\mathrm{km\,s^{-1}}$) assumed initially to exist in SEECHOs was not found at that time. After a 1 year interruption spent searching for possible artefacts and errors in the measuring equipment, improvements in the detector and the data-processing techniques, and long control experiments, the observations were resumed at the very end of March 2001.

It was found that these new data no longer reproduced the results obtained in March 2000. However, a more comprehensive analysis taking into account the shape of the scintillations permitted us to reveal, in both previous and new data, clear indications of the existence of a high-velocity population, which may be related both to the SEECHOs and to a daemon flux

from the Galactic disc (or their sum; detection in the future of seasonal variations in the intensity of these components will hopefully permit their discrimination). One detected also an extremely slow (3–5 km s^{-1}) population, which can exist only in GESCOs. Further, the data accumulated in the April–June 2001 period show unambiguously a gradual evolution of the GESCO population toward a slowing down of their velocity by 30–40% per month; that is, they gradually become confined within the Earth (which permits one, by the way, to estimate the force with which the material of the Earth decelerates the daemons). The fast evolution of the GESCO population with time offers an explanation for the absence in April 2001 of any indication of the NEACHO population, which was seen clearly in March 2000. The Earth apparently passed at that time through the 'shadow' produced by the Sun in the incoming Galactic disc population. In this shadow should be located the aphelia of the SEECHO population, and here, near the Earth' orbit, the NEACHOs created by the repeated action of the Earth on the SEECHO objects cross. The passage of this zone, where the Earth transfers daemons from the NEACHO population to the GESCOs, can take little time, not more than 1–2 months. In order to construct a final scenario of the orbital evolution of daemons and of their transfer from one population to another, round-the-year observations are naturally needed. It may, however, be conjectured even at this time that the passage in September through the weaker daemon 'antishadow' may permit one to observe one more antipodal NEACHO population.

An analysis of the possible processes on the atomic and subnuclear levels initiated by daemons in the components of our detector permitted us to make numerical estimates of some parameters characteristic of these processes.

For instance, Auger electrons are ejected from a daemon-captured atom in about 10^{-10} s, and their energies range from about 10 keV to about 0.6–1 MeV.

The de-excitation time of a nucleus captured by a daemon in ZnS(Ag) turns out to be somewhat shorter than 10^{-9} s. The characteristic excitation energies constitute several tens megaelectronvolts, and the excitation itself is removed by evaporation of nucleons and their clusters, which create extended scintillations.

Finally, we have refined the value of the decay time of a daemon-containing proton. It is $\Delta\tau_{ex} \approx 1\mu s$. Because the daemon is a relativistic object on a Planckian scale, this quantity is significant for the construction and experimental testing of the future quantum gravity theory.

References

Barrow, J. D., Copeland, E. J. and Liddle, A. R. (1992). *Phys. Rev. D*, **46**, 645.

Birks, J. B. (1964). *The Theory and Practice of Scintillation Counting.* Pergamon, Oxford.

Bauer, D. A. (1998). In: Roszkowski, L. (Ed.), *Proceedings of the Conference COSMO, 1997.* World Scientific, Singapore, pp. 140–154.

Drobyshevski, E. M. (1996). *Mon. Not. R. Astron. Soc.*, **282**, 211.

Drobyshevski, F. M. (1997a). In: Klapdor-Kleingrothaus, H. V. and Ramachers, Y. (Eds.), *Dark Matter in Astro- and Particle Physics.* World Scientific, pp. 417–424.

Drobyshevski, E. M. (1997b). *Proceedings of the 5th International Symposium on Ball Lightning*, Tsugawa Town, Japan, August 26–29, 1997, pp. 157–161.

Drobyshevski, E. M. (2000a). *Mon. Not. R. Astron. Soc.*, **311**, L1.

Drobyshevski, E. M. (2000b). *Phys. Atom. Nuclei*, **63**, 1037.

Drobyshevski, E. M. (2000c). astro-ph/0008020.

Drobyshevski, E. M. (2001). In: Churyumov, K. I. (Ed.), *Proceedings of the 4th Vsekhsvyatsky Readings*, Kiev University, Kiev, pp. 102–113 (in Russian).

Drobyshevski, E. M. (2002). *Astron. Astrophys. Trans.* **21**, 65.

Freese, K., Friemann, J. and Gould, A. (1988). *Phys. Rev. D*, **37**, 3388.

Markov, M. A. (1965). *Progr. Theor. Phys. Osaka, Suppl.*, 85.

Smirnov, B. M. (1990). *Soviet Phys. Usp.*, **33**, 261.

Spooner, N. J. C. (1998). In: Roszkowski, L. (Ed.), *Proceedings of the Conference COSMO*, World Scientific, Singapore, pp. 155–171.